Measurements of α-factor in 2–2.5 μm type-I In(Al)GaAsSb/GaSb high power diode lasers

L. Shterengas,[a] G. L. Belenky, and A. Gourevitch
State University of New York at Stony Brook, Stony Brook, New York 11794-2350

J. G. Kim and R. U. Martinelli
Sarnoff Corporation, CN5300, Princeton, New Jersey 08543-5300

(Received 5 August 2002; accepted 21 October 2002)

Spectra of the linewidth enhancement factor (α) of room-temperature-operated high-power 2–2.5 μm In(Al)GaAsSb/GaSb type-I quantum-well (QW) lasers were measured using Hakki–Paoli technique. Values of α at threshold were in the range 2.5 to 4 for all devices under study. Devices emitting 1 W cw power at $\lambda = 2.5$ μm have 1.5%–1.6% compressively strained QW active region and the lowest α equal to 2.5. Measured average filament spacings in near field are in rough agreement with predictions given by experimental α-factor values. © *2002 American Institute of Physics.* [DOI: 10.1063/1.1528291]

Mid-infrared laser applications like remote trace-gas monitoring, IRCM, LIDAR, and secure communications require either coherent sources with narrow linewidths or low divergence output beams. The parameter affecting both minimum spectral linewidth and beam quality is the α-factor, also called the linewidth enhancement factor or antiguiding parameter. The α-factor is the ratio of the derivatives with respect to the carrier concentration of the real and imaginary parts of the media complex dielectric function. In terms of measurable quantities, it is proportional to the ratio of changes in the refractive index and modal gain with injection current. For semiconductor lasers, any changes in the modal effective refractive index causes undesirable waveguide modification and, consequently, devices with low α are preferable. Typical values of the α-factor for semiconductor diode lasers are from 3 to 6.[1] However, smaller values were predicted and reported for doped/strained[2–4] and type-II[1,5] quantum-well (QW) devices.

High-power operation of type-I QW GaSb-based broad stripe lasers and single-mode operation of ridge devices have been reported.[6–8] In this work, we have measured the current dependences of the α-factor spectrum of type-I 2–2.5 μm In(Al)GaAsSb/GaSb diode lasers operating in a cw regime at room temperature. The α-factors at threshold are in the range 2.5 to 4, and are in agreement with α-factor values obtained from above-threshold near-field data showing filamentation. The measured linewidth enhancement factor for lasers with $\lambda = 2.5$ μm and ~1.5%–1.6% compressive strain in the QWs was 2.5, while devices with $\lambda = 2$ and 2.3 μm and lower strain (~1%) demonstrate larger α-factors.

The laser heterostructures were grown by molecular-beam epitaxy. The cladding layers are 2-μm-thick $Al_{0.9}Ga_{0.1}As_{0.07}Sb_{0.93}$. The separate confinement heterostructure and barrier layer composition is $Al_{0.25}Ga_{0.75}As_{0.02}Sb_{0.98}$. The laser emission wavelength was controlled by width (d) and composition of two InGaAsSb QWs. To keep the QW material out of the miscibility gap,[9,10] the QW compressive strain was higher for 2.5 μm (1.5%–1.6%, $d = 14.5$ nm) lasers than for the 2 and 2.3 μm devices (about 0.9% and 1.1%, respectively, $d = 22$ nm). To minimize the optical loss, the broadened waveguide (BW) laser design was used with total waveguide width W ranging from 830 to 840 nm. The BW approach reduced overlap of the optical field with doped cladding layers to 30%–35%, keeping QW confinement at about 3%. As a result, optical losses for all devices were as low as 2–4 cm^{-1}.

The wafers were processed into 100-μm-stripe, 1-mm-long lasers, the facets were anti/high-reflection coated (0.03/0.95), and the devices were mounted p-side down on Cu heatsinks. Low optical loss in combination with low series resistance led to 1 W cw and 5 W pulsed operation of $\lambda = 2.5$ μm lasers at room temperature. For details see Ref. 8.

Spectra of the α-factor were obtained from the current dependence of the amplified spontaneous emission (ASE) measured from the laser front facet. A spatial filtering technique[11,12] was used to filter out ASE of the on-axis mode of 100-μm-stripe width multimode lasers. ASE emission was measured in pulses (100 ns, 1 MHz) in order to minimize effect of Joule heating on laser characteristics.

Figure 1 shows the modal gain spectra of 2, 2.3, and 2.5 μm lasers at 20 °C for several currents below threshold (I_{th}), $I_{th} = 450$ mA (400–450 A/cm^2) for all devices under study. Increasing gain corresponds to increasing current. We used

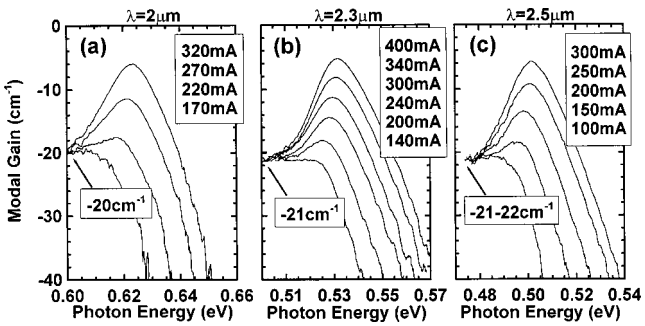

FIG. 1. Modal gain spectra for 2 μm (a), 2.3 μm (b), and 2.5 μm (c) lasers at 20 °C for different currents below threshold.

[a]Electronic mail: leon@ece.sunysb.edu

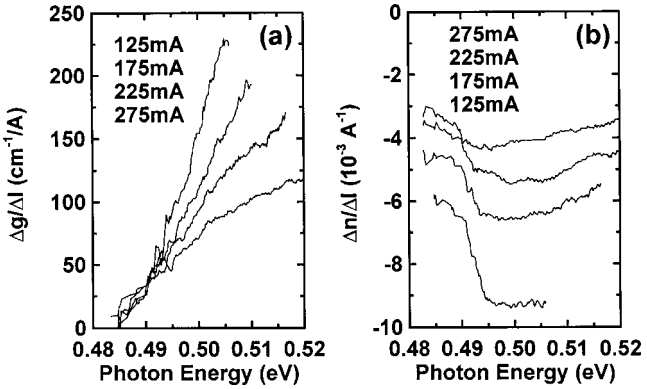

FIG. 2. Current dependences of the differential gain (a) and differential index (b) for 2.5 μm laser at 20 °C.

the Hakki–Paoli method to obtain these data from the ASE spectrum at each specified current.[13] At low energies the spectra converge, for the optical gain at sub-bandgap energies is zero at any current. As indicated in Fig. 1, the modal gain in low-energy limit equals the total loss[14] of 20–22 cm^{-1} for all devices. Subtracting from this value the mirror losses, which are about 18 cm^{-1}, leaves a value for internal loss of 2–4 cm^{-1}.

The differential gain ($\Delta g/\Delta I$) values were calculated from the data presented in Fig. 1. An example of the current dependence of the differential gain spectra is shown in Fig. 2(a) for a 2.5 μm laser. The corresponding differential index ($\Delta n/\Delta I$) was found through measurements of the relative shift of the Fabry–Perot modes with injection-current variations [Fig. 2(b)]. The effect of the Joule heating was controlled by measuring the rate of the laser line shift after the threshold. Carrier lifetime decrease with increasing concentration contributes to the observed reduction of $\Delta g/\Delta I$ and $\Delta n/\Delta I$ with injection current.

Figure 3 shows the α-factor spectra measured at different currents for 2, 2.3, and 2.5 μm lasers at 20 °C. The value of the α decreases with photon energy increase due to differential gain enhancement. The closer the electron is to the quasi-Fermi level, the higher is the differential gain for corresponding photon. The differential gain reaches its maximum at the photon energy $E=(m_c/m_r)E_{fc}+E_g$,[2] where m_c and m_r are the electron and reduced effective masses, respectively, E_{fc} is the electron quasi-Fermi level, and E_g is the energy gap.

Lasers emitting at 2 and 2.3 μm have α equal to 3.3 and

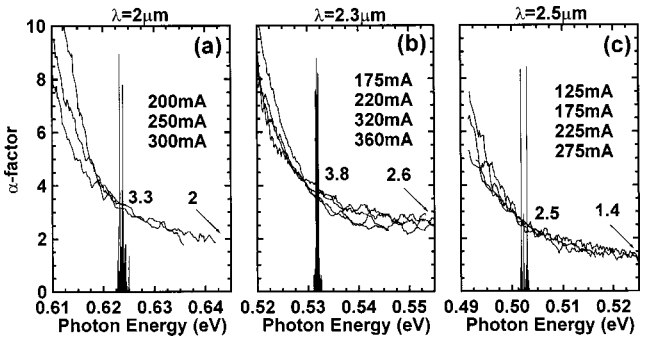

FIG. 3. Linewidth enhancement factor spectra for 2 μm (a), 2.3 μm (b), and 2.5 μm (c) lasers at 20 °C for different currents below threshold. Spectra of the laser emission just after threshold are shown in each laser for reference.

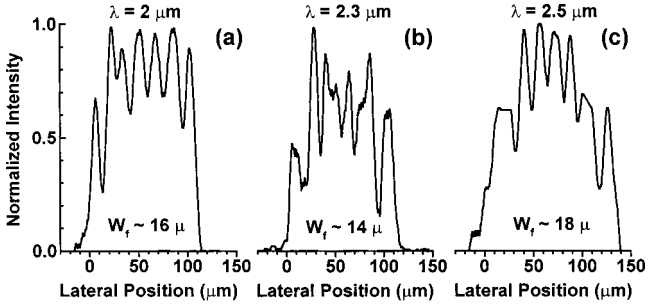

FIG. 4. Lateral near-field patterns measured $I\sim 3I_{th}$ for 2 μm (a), 2.3 μm (b), and 2.5 μm (c) lasers at 20 °C.

3.8, respectively, while 2.5 μm devices have smaller value of $\alpha=2.5$. As indicated by arrows in Fig. 3, the minimum values of α measured are 2, 2.6, and 1.4 for 2, 2.3, and 2.5 μm lasers, respectively. The lower value of α-factor for 2.5 μm, comparing to 2 and 2.3 μm devices, could be attributed to the higher compressive strain incorporated in the QW region (1.5%–1.6% versus about 1%) and smaller QW width (14.5 nm versus 22 nm) of 2.5 μm laser structure. Compressive strain and quantum confinement reduce the heavy hole effective mass. Decrease of the heavy hole effective mass moves quasi-Fermi levels closer to the electron states coupled to the laser mode, thereby increasing differential gain at the lasing wavelength. Differential refractive index can also increase with compressive strain, but to a lesser extent compared to differential gain.[4] Careful theoretical study taking into account free carrier effects[15] is required to understand details of α-factor dependence on strain and concentration.

An independent test for the value of the linewidth enhancement factor or antiguiding parameter was performed based on near-field pattern measurements. Total loss (γ) and α-factor determine the laser average filament spacing $W_F<[(\pi\lambda)/(\alpha\gamma n_{\text{eff}})]^{0.5}$,[16] where n_{eff} is the modal effective refractive index. Measurements of the current dependence of ASE allows for determination of all required parameters to estimate W_F. The estimated maximum average filament spacings were 16, 16, and 20 μm for 2, 2.3, and 2.5 μm lasers, respectively. Figure 4 shows near-field patterns measured after threshold and demonstrates that filamentation occurs for all devices studied. Average filament spacings were measured to be 16, 14, and 18 μm for 2, 2.3, and 2.5 μm lasers, respectively, that are in rough agreement with estimations according to Ref. 16; however, filaments in the middle of the contact stripe are more closely spaced (Fig. 4).

Summarizing, we have directly measured the spectra of the α-factor in type-I QW GaSb-based high-power lasers. Devices emitting at 2 and 2.3 μm, and having compressively strained quantum wells of about 1%, have α-factors of 3.3 and 3.8, respectively. Lasers emitting at 2.5 μm that have more heavily strained (~1.5%) quantum wells have an α-factor of 2.5. Near-field emission patters show filamentation, and average filament spacing values are in rough agreement with estimations based on measured internal losses and α-factors.

The authors thank Dr. M. Kisin for technical discussions. We also acknowledge the support from the United States Air Force Office of Scientific Research, Grant No. F-49620-01-10108, and from the Air Force Research Laboratory, Di-

rected Energy Directorate, Contract No. F29601-00-C-0003.

[1] J. T. Olesberg, M. E. Flatte, and T. F. Boggess, J. Appl. Phys. **87**, 7164 (2000).
[2] T. Yamanaka, Y. Yoshikuni, K. Yokoyama, W. Lui, and S. Seki, IEEE J. Quantum Electron. **29**, 1609 (1993).
[3] H. Mawatari, F. Kano, N. Yamamoto, Y. Kondo, Y. Tohmori, and Y. Yoshikuni, Jpn. J. Appl. Phys., Part 1 **33**, 811 (1994).
[4] A. Schonfelder, S. Weisser, J. D. Ralston, and J. Rosenzweig, IEEE Photonics Technol. Lett. **6**, 891 (1994).
[5] S. A. Anson, J. T. Olesberg, M. Flatte, and T. C. Hasenberg, J. Appl. Phys. **86**, 713 (1999).
[6] D. V. Donetsky, D. Westerfeld, G. L. Belenky, R. U. Martinelli, D. Z. Garbuzov, and J. C. Connolly, J. Appl. Phys. Com. **90**, 4281 (2001).
[7] D. Garbuzov, R. Menna, M. Maiorov, H. Lee, V. Khalfin, L. DiMarco, D. Capewell, R. Martinelli, G. Belenky, and J. Connolly, Proc. SPIE **3628**, 124 (1999).
[8] J. G. Kim, L. Shterengas, R. U. Martinelli, G. L. Belenky, D. Z. Garbuzov, and W. K. Chan, Appl. Phys. Lett. **81**, 3146 (2002).
[9] K. Shim, H. Rabitz, and P. Dutta, J. Appl. Phys. **88**, 7157 (2000).
[10] V. S. Sorokin, S. V. Sorokin, A. N. Semenov, B. Ya. Meltser, and S. V. Ivanov, J. Cryst. Growth **216**, 97 (2000).
[11] D. J. Bossert and D. Gallant, Electron. Lett. **32**, 338 (1996).
[12] D. V. Donetsky, G. L. Belenky, D. Z. Garbuzov, H. Lee, R. U. Martinelli, G. Taylor, S. Luryi, and J. C. Connolly, IEEE Electron Device Lett. **35**, 298 (1999).
[13] B. W. Hakki and T. L. Paoli, J. Appl. Phys. **44**, 4113 (1973).
[14] L. J. P. Ketelsen, IEEE Electron Device Lett. **30**, 1422 (1994).
[15] H. Wenzel, G. Erbert, and P. M. Enders, IEEE J. Sel. Top. Quantum Electron. **5**, 637 (1999).
[16] D. Mehuys, R. J. Lang, M. Mittelstein, J. Salzman, and A. Yariv, IEEE J. Quantum Electron. **23**, 1909 (1987).